High-resolution dynamic computer simulation analysis of the behavior of sample components with pI values outside the pH gradient established by carrier ampholyte capillary isoelectric focusing

Wolfgang Thormann[1*], Ferenc Kilár[2]

[1] Clinical Pharmacology Laboratory, Institute for Infectious Diseases, University of Bern, Murtenstrasse 35, CH-3010 Bern, Switzerland.

[2] Institute of Bioanalysis, Faculty of Medicine, University of Pécs, Pécs, Hungary

Running title: Samples outside pH gradient in carrier ampholyte isoelectric focusing

Keywords: simulation, isoelectric focusing, sample application, carrier ampholytes, isotachophoresis

Abbreviations: CIEF, capillary isoelectric focusing

* author to whom correspondence should be addressed:

Prof. Dr. Wolfgang Thormann

Clinical Pharmacology Laboratory, Institute for Infectious Diseases, Murtenstrasse 35
CH-3010 Bern, Switzerland
phone: +41 31 632 3288; fax: +41 31 632 4997 ; email: wolfgang.thormann@ifik.unibe.ch

Received: September 11, 2012; Revised: October 26, 2012; Accepted: October 30, 2012

Abstract

The behavior of sample components whose pI values are outside the pH gradient established by 101 hypothetical biprotic carrier ampholytes covering a pH 6-8 range was investigated by computer simulation under constant current conditions with concomitant constant electroosmosis towards the cathode. Data obtained with the sample being applied between zones of carrier ampholytes and on the anodic side of the carrier ampholytes were studied and found to evolve into zone structures comprising three regions between anolyte and catholyte. The focusing region with the pH gradient is bracketed by two isotachopheretic zone structures comprising selected sample and carrier components as isotachophoretic zones. The isotachophoretic structures electrophoretically migrate in opposite direction and their lengths increase with time due to the gradual isotachophoretic decay at the pH gradient edges. Due to electroosmosis, however, the overall pattern is being transported towards the cathode. Sample components whose pI values are outside the established pH gradient are demonstrated to form isotachophoretic zones behind the leading cation of the catholyte (components with pI values larger than 8) and the leading anion of the anolyte (components with pI values smaller than 6). Amphoteric compounds with appropriate pI values or non-amphoteric components can act as isotachophoretic spacer compounds between sample compounds or between the leader and the sample with the highest mobility. The simulation data obtained provide for the first time insight into the dynamics of amphoteric sample components which do not focus within the established pH gradient.

1 Introduction

Isoelectric focusing (IEF) is a high-resolution technique for separation and analysis of amphoteric sample components in a pH gradient which increases from anode to cathode [1-6]. Capillary IEF (CIEF) with commercial carrier ampholytes as separation medium is the instrumental format of this technique. For CIEF in quiescent solution, either an array or scanning detector has to be employed, or the sample pattern must be mobilized either during or following focusing such that analytes can be detected as they pass an on-column (absorbance of fluorescence) or be swept into an end-column (MS) detector. Mobilization can be accomplished by electrophoresis, electroosmosis, imposed hydrodynamic flow, or any combination of these principles [7-18].

Dynamic computer simulation of IEF in presence of carrier ampholytes has demonstrated considerable value as a research tool [3,19]. Simulations performed with the one dimensional model GENTRANS have been used to predict separation dynamics of low and high molecular mass amphoteric components, pH gradient formation and stability, and electrophoretic mobilization during and after focusing. These studies revealed that focusing is composed of two phases, a fast separation phase and a very slow stabilizing phase, whereas electrophoretic mobilization and decay processes occurring at the pH gradient interfaces with the anolyte and the catholyte are of isotachophoretic nature [20-29]. The same simulator was also used to study the nature and impact of EOF under focusing conditions [30-32]. Focusing in a microchannel with variable cross-sectional area was investigated with a modified one dimensional mass transport model [33]. A two dimensional simulation model was used to study focusing in microgeometries of uniform and changing cross-sections [34], the effect of ionic strength on mobilities of carrier ampholytes [35] and dispersion of protein bands in a horseshoe microchannel [36].

In carrier ampholyte based focusing, sample components are typically applied as a zone mixed with the carrier ampholytes. Other sampling strategies, including sample application as a short zone within the initial carrier ampholyte zone, sandwiched in absence of carrier ampholytes between zones of carrier ampholytes or before a zone comprising carrier ampholytes, were studied recently in order to establish optimized sampling conditions for CIEF with electroosmotic mobilization and detection towards or at the cathodic capillary end [32]. Simulation data obtained suggested that sample placed at the anodic side or end of the initial carrier ampholyte zone are the favorable configurations for CIEF with electroosmotic zone mobilization. Focusing of seven amphoteric sample components in a broad range pH

gradient (pH 3-11) composed of 101 carrier ampholytes was investigated under constant voltage conditions. The pI values of the sample components were within the pH gradient established by the carrier ampholytes [32]. As a continuation of that work, the electrophoretic behavior of the same seven sample components for a narrow range pH gradient (pH 6-8) was investigated. Two sampling possibilities, namely with the sample being applied as short zone (i) between zones of carrier ampholytes and (ii) on the anodic side of the carrier ampholytes, were studied. The thereby obtained data and gained insights are presented in this paper. With the narrow pH gradient, three of the seven sample components had pI values outside the pH gradient which permitted the detailed study of the electrophoretic behavior of these components under the influence of the electric field strength. For the sake of data comparison, simulations were performed under constant current and constant EOF conditions. The simulation data obtained provided for the first time insight into the behavior of amphoteric sample components which do not focus within the established pH gradient. This work was conducted in the context of developing strategies for CIEF-MS which are part of ongoing research activities at the University of Pécs [13,17,18].

2 Experimental

2.1 Computer simulations

The previously described high-resolution transient PC-based model GENTRANS in which electroosmosis is considered to be a plug flow was employed [19,30-32]. The isothermal model is one dimensional, based upon the principles of electroneutrality and conservation of mass and charge, and component fluxes are computed on the basis of electromigration, diffusion and plug flow (electroosmosis). Initial conditions which must be specified include the distribution of all components, the pKa values of the buffer and sample constituents, the mobility values of the neutral and charged species of the small molecular mass components, the input data for electroosmosis, the magnitudes of constant voltage or constant current density, the duration of power application, the column length as well as its segmentation and the species permeabilities (boundary conditions) at the ends of the separation space. The program outputs concentration, pH, conductivity, ionic strength and flow distributions along the uniform separation channel. The distribution of other parameters, including the electric field strength which equals current density divided by conductivity, can be calculated from the outputted data.

2.2 Input data and execution of simulations

A 10 cm focusing space divided into 10000 segments of equal length, a constant 100 μm/s EOF and constant current density of 250 A/m^2 were employed. 101 hypothetical biprotic carrier ampholytes were used to establish a pH gradient between anode and cathode. Their pI values uniformly span the range 6.00-8.00 ($\Delta pI = 0.02$). For each ampholyte, ΔpK was 2.5, the ionic mobility was 2.5×10^{-8} m^2/Vs and the initial concentration was 0.2 mM. These carrier ampholyte conditions are similar to those employed previously for the simulation of focusing and electrophoretic mobilization of hemoglobin variants [26,28]. The sample was composed of 7 amphoteric components with pI values 5.3, 6.4, 6.6, 7.2, 7.9, 8.6 and 10.4 and HCl. Initially, the overall sample and carrier ampholyte zones occupied 20 % of total column length (arranged at anodic column end from 3 to 23 % of column length; diffusion boundaries 0.001 %). Two configurations were analyzed with the sample applied as a short zone either between zones of carrier ampholytes (referred to as sandwich sampling [13,32]) or on the anodic side of carrier ampholytes (referred to as half-sandwich [17,32]). In both cases, the sample did not comprise carrier ampholytes and occupied 2 % of column length (2 mm effective length). The sandwich sampling example essentially represents the configuration of Figure 4d in Ref. 13. Physico-chemical input data are presented in Table 1. 10 mM phosphoric acid and 20 mM NaOH served as anolyte and catholyte, respectively. All simulations were performed with an open cathodic column end, which allows mass transport into and out of the separation space, and constant boundary conditions at the anodic column end [32]. The program was executed on PC's featuring Pentium IV and i5 processors running at frequencies between 1.9 and 2.4 GHz. For making plots, simulation data were imported into SigmaPlot Scientific Graphing Software version 10 (SPSS, Chicago, IL, USA).

3 Results and discussion

3.1 Formation of the pH gradient

Focusing of 101 hypothetical ampholytes forming a pH 6 to 8 gradient and seven amphoteric sample components between 20 mM NaOH (catholyte) and 10 mM phosphoric acid (anolyte) was investigated using GENTRANS. For the sake of comparison of the developed electrophoretic patterns, simulations were performed at constant current density and constant cathodic EOF. Two configurations were analyzed. In the first one the sample was applied between carrier ampholyte zones of 6 and 12 mm length (Figure 1; sandwich arrangement) whereas in the second case the sample was on the anodic side of an 18 mm long carrier

ampholyte zone (Figure 2; half sandwich arrangement). In both cases, the initial positions of anolyte end and catholyte boundaries were at 3 and 23 %, respectively, of the column length. Simulations were run for up to 10 min of power application and required several days for completion.

Upon power application, separation of carrier and sample components occurred together with concomitant displacement of the entire zone structure towards the cathode provided by the applied constant cathodic plug flow. The separation of the carrier components has been described previously for various configurations [20,21,23,26] and is therefore not shown here. Carrier components become concentrated and aligned according to their pI values, with the most acidic carrier on the anodic side and the most alkaline carrier component on the cathodic side thereby establishing a pH gradient which increases from anode (pH 6) to cathode (pH 8). Focusing of carrier ampholytes is complete within about 4 min (data not shown). Distributions of all components after 5 min of current application are presented in panels A of Figures 1 and 2. Distributions of sample components together with the pH and electric field strength profiles for the same time point are depicted in panels B of both figures. The carrier components are predicted to become concentrated to about 10 mM (about 50-fold concentration) and there is a small decrease in their concentrations at the locations of focused sample components. Having the sample between two zones of carrier ampholytes produces a gap within the fluid element that was originally occupied by the sample. The gap is characterized with a smaller carrier ampholyte concentration, a shallower pH gradient and an area of lower conductivity and thus higher electric field strength (Figure 1, marked with asterisks). The gap somewhat delays the focusing process of the carrier ampholytes around its location and remains persistent upon prolonged application of power (data not shown), which is consistent with the results previously shown for another configuration [32].

The data presented in Figures 1 and 2 reveal that the positions of the phosphoric acid and sodium boundaries are identical. This does not come as a surprise as both simulations were performed at the same constant current density and the same constant EOF. The same is true for the cathodic end of the pH gradient. This end is marked by a large change in the electric field strength and thus conductivity. On the anodic side of the established pH gradient, however, the positions of the gradient edges are not equal. For the case having the initial sample between two zones of carrier ampholytes (Figure 1), the position of the gradient edge is more towards the anode compared to the case with the sample placed on the anodic side of the initial carrier ampholyte zone (Figure 2). The reason is a distribution of the gradient over a

longer part of the capillary which also includes the part of the initial sample zone. As a consequence thereof, the pH gradient on the anodic side becomes somewhat shallower which has an impact on the focusing of sample components in this region (see below). Thus, although the same amounts of carrier ampholytes were sampled in both cases, the established pH gradients are not identical. This should be kept in mind when sandwich sampling is employed.

3.2 Dynamics of sample components

The data presented in Figure 3 depict the dynamics of the sample components for 0, 1, 2, 4 and 8 min of current flow. For the case of sandwich sampling (Figure 3A), sample separation becomes complete shortly after 2 min. With the other configuration, the separation of the sample components is much faster (Figure 3B) which is in agreement with the recent study published with a configuration featuring a broad range pH gradient [32]. Except for the location of the pH gradient on the anodic side of the gap, the predicted sample component profiles are identical. This is shown with the 8 min data presented in Figure 3C in which the distributions and locations of the pI 5.3, 7.2, 7.9, 8.6 and 10.4 sample components are identical whereas the positions of the pI 6.4 and 6.6 samples are different. The same is the case after 5 min (Figures 1 and 2) and 4 min (Figure 3) of current flow. At earlier time points, not all sample components have reached their focusing positions (Figure 3).

The dynamics of the seven sample components within the first minute of power application are presented in Figure 4. First, separation of the sample components occurs in a manner similar to zone electrophoresis with the exception that separation is taking place in a non-uniform environment which changes with time [32]. In the case of the half sandwich, all except the pI 5.3 sample component enter as cations the carrier ampholyte zone and separate rapidly (within about 0.4 min, Figure 4B). Once the pI 10.4 and 8.6 components reached the cathodic end of the carrier ampholyte zone, their isotachophoretic zones begin to form. These isotachophoretic zones are predicted to be complete after 0.8 min and occur via a transient peak splitting mechanism (seen e.g. at 0.6 min for pI 8.6 component, Figure 4B). On the other side, the pI 5.3 component immediately starts to form its anionic isotachophoretic zone. In the case of sandwich sampling (Figure 4A), the pI 7.2, 7.9, 8.6 and 10.4 components enter as cations the carrier ampholyte zone on the cathodic side of the applied sample whereas the pI 5.3, 6.4 and 6.6 components migrate as anions into the carrier ampholyte zone on the anodic side of the sample. Except for the pI 6.4 and 6.6 components, separation occurs quickly (less than 0.4 min, Figure 4A). The two cationic isotachophoretic zones are predicted to become

established somewhat earlier compared to those of Figure 4B because the length of the carrier ampholyte zone through which migration has to occur is shorter in the case of sandwich sampling. The opposite is true for the formation of the anionic isotachophoretic zone of the pI 5.3 sample component (Figure 4). Transient peak splitting is predicted for all ampholytes which form an isotachophoretic zone (shown for the pI 5.3 and the 8.6 components at 0.4 min in Figure 4A).

Four of the seven sample components, the pI 6.4, 6.6, 7.2 and 7.9 components, have pI values which correspond to pH values within the pH gradient and thus become focused according to the principles of isoelectric focusing forming peaks with Gaussian distributions (Figure 3C, panels B of Figures 1 and 2). Not surprisingly, as the sample components have unequal ΔpK values and were sampled with unequal amounts (Table 1), focused peak shapes are different. Three of the sample components have pI values outside the established pH gradient and thus do not become focused within the pH gradient. Instead, the pI 5.3, 8.6 and 10.4 sample components form isotachophoretic zones with characteristic plateau concentrations, pH values and conductivities (Figures 1B, 2B and 3C). The pI 5.3 compound forms an anionic ITP zone on the anodic side of the pH gradient directly behind phosphoric acid (Figures 1A and 2A). It is followed by the gradual removal of the most acidic carrier ampholytes (see components with pI values of 6.00 and 6.02 in panels A of Figures 1 and 2) which are part of the isotachophoretic decay process which occurs at the anodic edge of the pH gradient and is in agreement with previous findings [22,26,28,32]. The ITP displacement rate towards the anode is equal to the velocity of the phosphoric acid boundary, $v_P = \mu_{eff(P)} I/\kappa_a$ where $\mu_{eff(P)}$, I and κ_a refer to the effective mobility of phosphoric acid, current density and conductivity of the anolyte, respectively. The values for the three parameters are 2.26 10^{-8} m^2/Vs, 250 A/m^2 and 0.2382 S/m, respectively, which results in a displacement rate of 23.72 μm/s. However, because of the EOF towards the cathode which is larger compared to the anodic ITP migration rate, the overall transport rate is towards the cathode and amounts to 76.28 μm/s (Figure 3). The pI 8.6 and 10.4 sample components form cationic ITP zones behind sodium on the cathodic side of the pH gradient and are followed immediately by the most alkaline carrier components (components with pI values of 8.00 and 7.98 in panels A of Figures 1 and 2). Their transport rate is the addition of the cathodic electrophoretic migration rate of the sodium boundary, $v_{Na} = \mu_{eff(Na)} I/\kappa_c$ where κ_c is the conductivity of the catholyte, and the EOF. The values for the three parameters are 5.19 10^{-8} m^2/Vs, 250 A/m^2 and 0.4837 S/m,

respectively, which results in an ITP displacement rate of 26.83 μm/s. The net transport towards the cathode is thus 126.83 μm/s (Figure 3).

Sample components whose pI values are within but close to one pH gradient edge first become focused which is demonstrated with the pI 7.9 component (Figure 3). Upon prolonged electrophoresis, however, such analytes are converted into migrating ITP zones as a result of the gradual decay of the pH gradient at its edges. The involved transport mechanism is the same as is shown for the first two carrier ampholytes in Figures 1 and 2 (pI 8.00 and 7.98 components on cathodic side and pI 6.00 and 5.98 components on anodic side, panels A of Figures 1 and 2). In the simulations presented in this paper, the amphoteric sample components were assumed to have ionic mobilities smaller than those of the carrier ampholytes. The use of equal or larger ionic mobilities compared to those of the carrier components would result in the same separations and thus provide comparable results. For the simulations with carrier component mobilities of 2.5×10^{-8} m^2/Vs, sample foci formed within the pH gradient are predicted to be independent of the ionic mobilities of the sample components. Transient states and isotachophoretic zone properties of the sample components, however, are dependent on ionic mobilities. This was studied with sample component mobilities ranging between 2.0×10^{-8} and 3.0×10^{-8} m^2/Vs (data not shown).

3.3 Isotachophoretic zone formation outside of the pH gradient

The isotachophoretic zone formation of the sample components occurs rapidly within the first minute of power application (Figure 4) and remained as isotachophoretic zones as is documented with the cationic data presented in Figure 5. After 0.5 min, the isotachophoretic zone of the pI 10.4 component is already fully established whereas the zone formation process for the pI 8.6 component is still ongoing. After 1 min of current flow, the zones of the two cationic sample components are predicted to have formed completely. After formation, the shapes of these two zones do not change but continue to migrate at the constant rate of 126.83 μm/s towards the cathode (compare with 2 and 4 min data of Figure 5). This is characteristic for ITP. The carrier ampholytes, however, are only partly separated at the 1 and 2 min time points. Their focused zones are fully established after about 4 min of current flow. The data presented in Figure 4 nicely visualize the gradual isotachophoretic removal of carrier ampholytes at the cathodic edge of the pH gradient. This occurs even further with prolonged electrophoresis.

The ITP formation of sample zones outside the pH gradient is also demonstrated with the addition of spacer compounds. The cationic data depicted in Figure 6 represent component distributions after 5 min of power application for the configuration of Figure 1 without (panel A) and with application of spacer compounds (panels B and C). Spacer compounds were added in the amounts of the carrier components as stated in Section 2.1. A pI 9.5 spacer which has a pI between the pIs of the two sample components, is shown to establish an ITP zone between the two sample components (Figures 6B and 6C) whereas a pI 11.0 spacer is forming an ITP zone between sodium (the leader) and the pI 10.4 sample component (Figure 6C). Such configurations are not unrealistic as commercial carrier ampholyte mixtures are not having a sharp pI edge but certainly also contain a number of additional components with larger and lower pI compared to those claimed for the product (probably in decreasing amounts compared to the components of the claimed gradient). Furthermore, non-amphoteric weak acids (on anodic side) and weak bases (on cathodic side) which are present in the sample or carrier ampholyte mixture can also act as ITP spacers provided their effective mobility is lower compared to the mobility of the leading ions. Strong ions with high mobility, such as chloride, typically do not fulfill this criterion and electrophoretically migrate into the leader in a zone electrophoretic way [32].

The data presented in this paper illustrate that current flow induces three regions between anolyte (phosphoric acid) and catholyte (NaOH). The focusing region is bracketed by two isotachophoretic zone structures comprising selected sample and carrier components as ITP zones. The electric field strength data presented in panels B of Figures 1 and 2 indicate that the electric field strength is higher across the ITP zone structures compared to the isoelectric focusing part. Both transitions between focusing and ITP regions are marked with a strong change in the electric field strength. Furthermore, the electric field strength across most migrating ITP boundaries is characterized by spikes (marked with # in panels B of Figures 1 and 2) which are comparable to those described by Mosher et al. [39]. The electric field strength within catholyte (NaOH) and anolyte (phosphoric acid) is very low (0.5169 kV/m and 1.0495 kV/m, respectively). ITP zone formation on either side of the pH gradient is independent of sample application. Thus, comparable patterns would also be obtained with an initial mixture of sample and carrier components.

4 Concluding remarks

Focusing of amphoteric sample components together with 101 hypothetical biprotic carrier ampholytes covering a pH 6-8 range was studied under constant current conditions with

concomitant constant electroosmosis towards the cathode using high-resolution computer simulation. Data obtained with the sample being applied between zones of carrier ampholytes and on the anodic side of the carrier ampholytes were studied and found to evolve into zone structures comprising three regions between anolyte and catholyte. The focusing region with the pH gradient is bracketed by two isotachophoretic zone structures comprising selected sample and carrier components as ITP zones. The ITP structures migrate in opposite direction away from the pH gradient and their lengths increase gradually. Sample components whose pI values are outside the established pH gradient are demonstrated to form ITP zones behind the leading cation of the catholyte (components with pI values larger than 8) and the leading anion of the anolyte (components with pI values smaller than 6) or between isotachophoretically migrating carrier components of the gradient edges. Furthermore, any amphoteric components with pI values outside those which form the focusing gradient or non-amphoteric components which migrate behind the leading ions can act as isotachophoretic spacers of sample components. Simulation work with other pH gradients and comparison with experimental results is currently being performed and will be reported in due time.

Acknowledgements

This work was supported by the Swiss NSF and by the grants TÁMOP 4.2.2./B-10/1-2010-0029 and OTKA K-100667.

Conflicts of interest

The authors have declared no conflict of interest.

5 References

[1] Rilbe, H., Ann. N. Y. Acad. Sci. 1973, 209, 11-22.

[2] Righetti, P.G., Isoelectric Focusing: Theory, Methodology and Applications, Elsevier, Amsterdam, 1983.

[3] Mosher, R.A., Saville, D.A., Thormann, W., The Dynamics of Electrophoresis, VCH Publishers, Weinheim, 1992.

[4] Hjertén, S., in Grossman, P.D., Colburn, J.C. (Eds.), Capillary Electrophoresis, Theory and Practice, Academic Press, San Diego, 1992, pp. 191-214.

[5] Righetti, P.G., Stoyanov, A.V., Zhukov, M.Y., The Proteome revisited, Theory and Practice of all relevant Electrophoretic Steps, Elsevier, Amsterdam, The Netherlands, 2001.

[6] Garfin, D., Ahuja, S., Eds., Handbook of Isoelectric Focusing and Proteomics, Elsevier, Amsterdam, The Netherlands, 2005.

[7] Hjertén, S., Zhu, M., J. Chromatogr. 1984, 346, 265-270.

[8] Hjertén, S., Liao, J., Yao, K., J. Chromatogr. 1987, 387, 127-138.

[9] Thormann, W., Caslavska, J., Molteni, S., Chmelík, J., J. Chromatogr. 1992, 589, 321-327.

[10] Caslavska, J., Molteni, S., Chmelík, J., Šlais, K., Matulík, F., Thormann, W., J. Chromatogr. A 1994, 680, 549-559.

[11] Rodriguez-Diaz, R., Wehr, T., Zhu, M., Electrophoresis 1997, 18, 2134-2144.

[12] Wu, J., Pawliszyn, J., Electrophoresis 1995, 16, 670-673.

[13] Kilár, F., Végvári, Á., Mód, A., J. Chromatogr. A 1998, 813, 349-360.

[14] Shimura, K., Electrophoresis 2002, 23, 3847-3857.

[15] Kilár, F., Electrophoresis 2003, 24, 3908-3916.

[16] Mack, S., Cruzado-Park, I., Chapman, J., Ratnayake, C., Vigh, G., Electrophoresis 2009, 30, 4049-4058.

[17] Páger, C., Dörnyei, Á., Kilár, F., Electrophoresis 2011, 32, 1875-1884.

[18] Páger, C., Vargová, A., Takácsi-Nagy, A., Dörnyei, Á., Kilár, F., Electrophoresis 2012, 33, in press (doi: 10.1002/elps.201200175).

[19] Thormann, W., Breadmore, M.C., Caslavska, J., Mosher, R.A., Electrophoresis 2010, 31, 726-754.

[20] Thormann, W., Mosher, R.A., Bier, M., J. Chromatogr. 1986, 351, 17-29.

[21] Mosher, R.A., Thormann, W., Kuhn, R., Wagner, H., J. Chromatogr. 1989, 478, 39-49.

[22] Mosher, R.A., Thormann, W., Electrophoresis 1990, 11, 717-723.

[23] Mao, Q., Pawliszyn, J., Thormann, W., Anal. Chem. 2000, 72, 5493-5502.

[24] Mosher, R.A., Thormann, W., Electrophoresis 2002, 23, 1803-1814.

[25] Thormann, W., Huang, T.M., Pawliszyn, J., Mosher, R.A., Electrophoresis 2004, 25, 324-337.

[26] Thormann, W., Mosher, R.A., Electrophoresis 2006, 27, 968-983.

[27] Mosher, R.A., Thormann, W., Electrophoresis 2008, 29, 1036-1047.

[28] Thormann, W., Mosher, R.A. Electrophoresis 2008, 29, 1676-1686.

[29] Steinmann, L., Mosher, R.A., Thormann, W., J. Chromatogr. A 1996, 756, 219-232.

[30] Thormann, W., Zhang, C.-X., Caslavska, J., Gebauer, P., Mosher, R.A., Anal. Chem. 1998, 70, 549-562.

[31] Thormann, W., Caslavska, J., Mosher, R.A., J. Chromatogr. A 2007, 1155, 154-163.

[32] Takácsi-Nagy, A., Kilár, F., Páger, C., Mosher, R.A., Thormann, W., Electrophoresis 2012, 33, 970-980.

[33] Chou, Y., Yang, R.-J., Electrophoresis 2009, 30, 819-830.

[34] Shim, J., Dutta, P., Ivory, C.F., Electrophoresis 2007, 28, 572-586.

[35] Shim, J., Dutta, P., Ivory, C.F., Electrophoresis 2008, 29, 1026-1035.

[36] Shim, J., Dutta, P., Ivory, C.F., Electrophoresis 2009, 30, 723-731.

[37] Šlais, K., Friedl, Z., J. Chromatogr. A 1994, 661, 249-256.

[38] Šlais, K., Friedl, Z., J. Chromatogr. A 1995, 695, 113-122.

[39] Mosher, R.A., Thormann, W., Bier, M., J. Chromatogr. 1985, 320, 23-32.

Figure 1: Computer predicted distribution of (A) all components and (B) sample components, pH and electric field strength after 5 min of current application. The initial configuration includes the sample containing 7 analytes sandwiched between two zones with unequal lengths each comprising a mixture of 101 carrier ampholytes which cover pI 6 to 8. The initial distribution is depicted in the insert of panel A, whereas the formed zones of the pI 8.6 and 10.4 sample components are shown as insert in panel B. Electrophoresis took place at a constant current density of 250 A/m^2 between 20 mM NaOH (catholyte) and 10 mM phosphoric acid (anolyte) and with a concomitant constant EOF of 100 μm/s towards the cathode. Asterisks mark the location of the carrier ampholyte gap. Electric field strength spikes across migrating ITP boundaries are marked with #. Numbers, S, CA, P and E refer to pI values, sample, carrier ampholytes, phosphoric acid and electric field strength, respectively. The cathode is to the right.

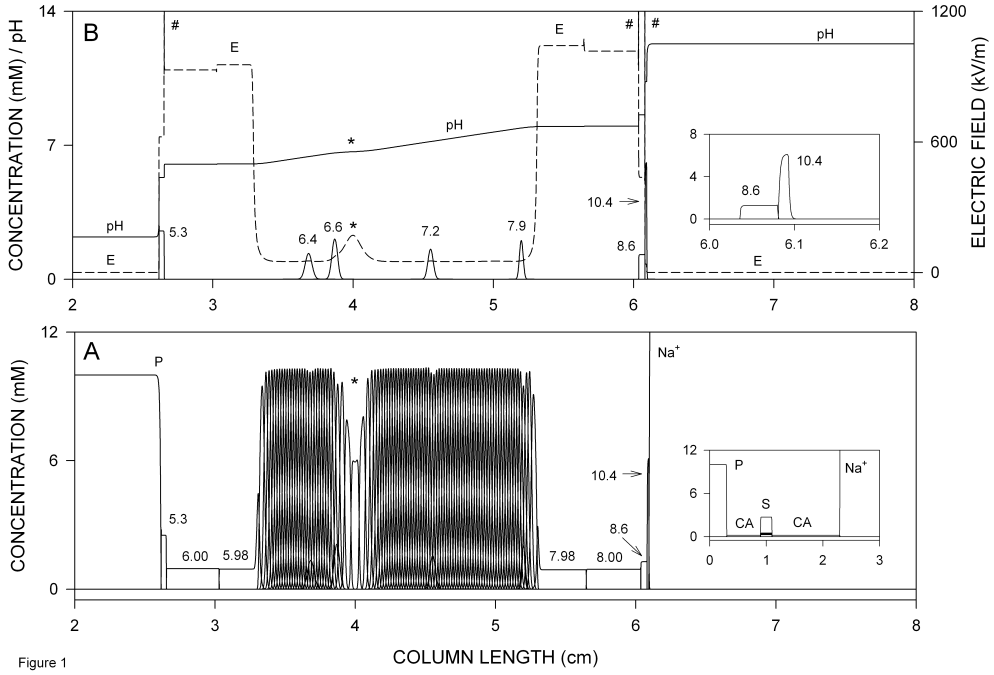

Figure 1

Figure 2: Computer predicted distribution of (A) all components and (B) sample components, pH and electric field strength after 5 min of current application to a configuration with the sample containing 7 analytes applied on the anodic side of the carrier ampholytes and otherwise identical conditions as for Figure 1.

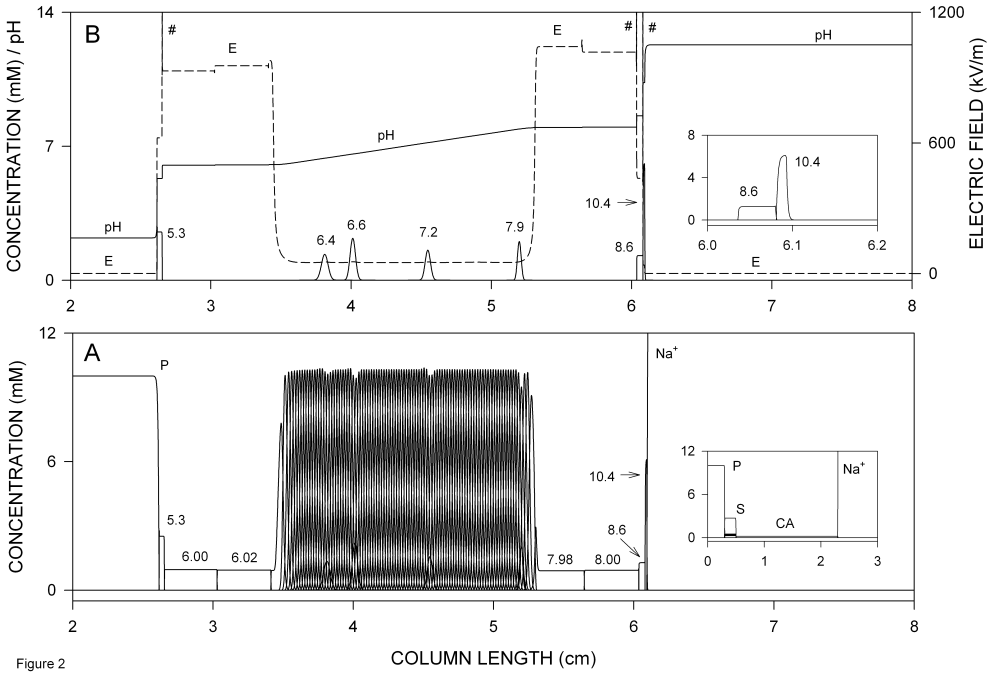

Figure 2

Figure 3: Computer predicted dynamics of sample components after 0, 1, 2, 4 and 8 min of power application for (A) sandwich and (B) half sandwich sample application. Data of successive time points are presented with a y-scale offset of 3 mM and initial distributions of all components are given as inserts. Panel C depicts the distributions of the sample components and pH after 8 min for the two cases with the data of the half sandwich presented as dotted lines. Numbers, P, S and CA refer pI values, phosphoric acid, sample and carrier ampholytes, respectively. The cathode is to the right.

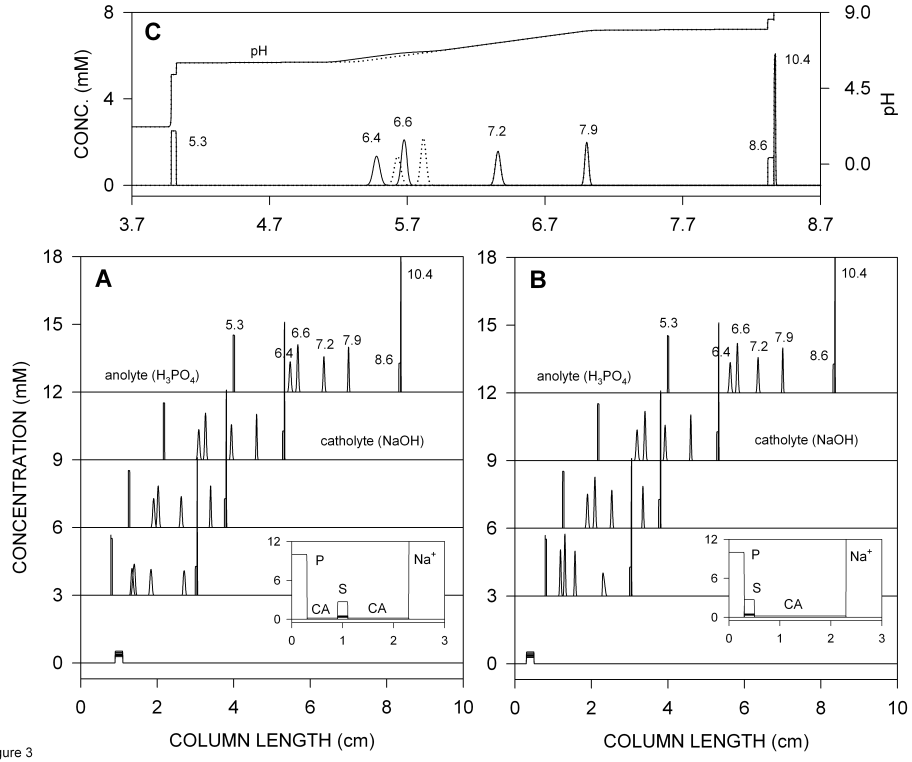

Figure 3

Figure 4: Computer predicted dynamics of sample components after 0, 0.2, 0.4, 0.6, 0.8 and 1.0 min of power application for (A) sandwich and (B) half sandwich sample application. Data are presented with a y-scale offset of 5 mM. Other conditions as for Figure 3.

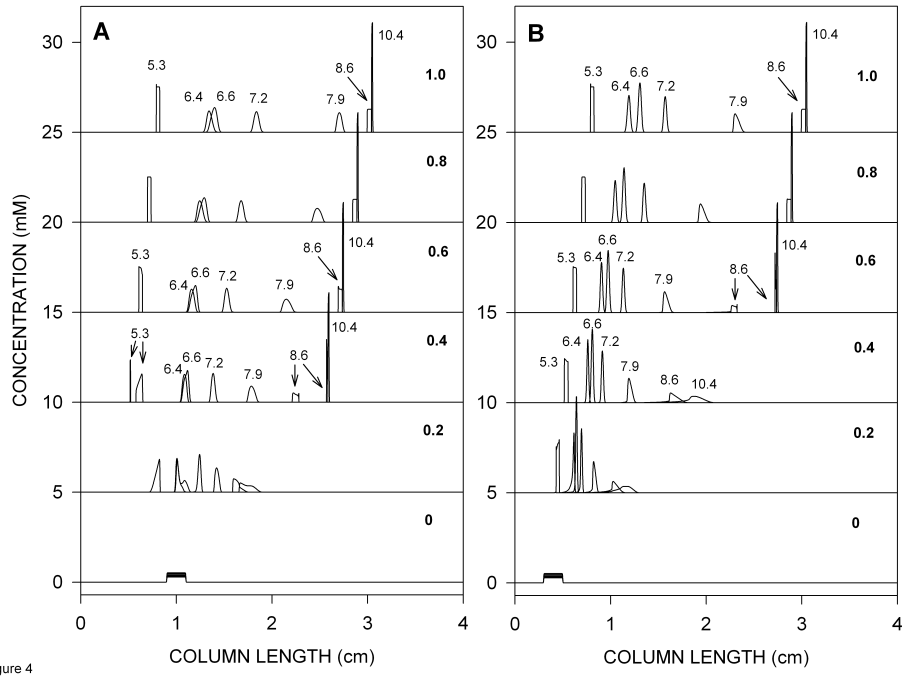

Figure 4

Figure 5: Computer predicted cathodic region showing the distribution of the compounds after 0.5, 1.0, 2.0 and 4.0 min of current application for the case of Figure 1. CA refers to carrier ampholyte and numbers indicate the pI of the components. The cathode is to the right.

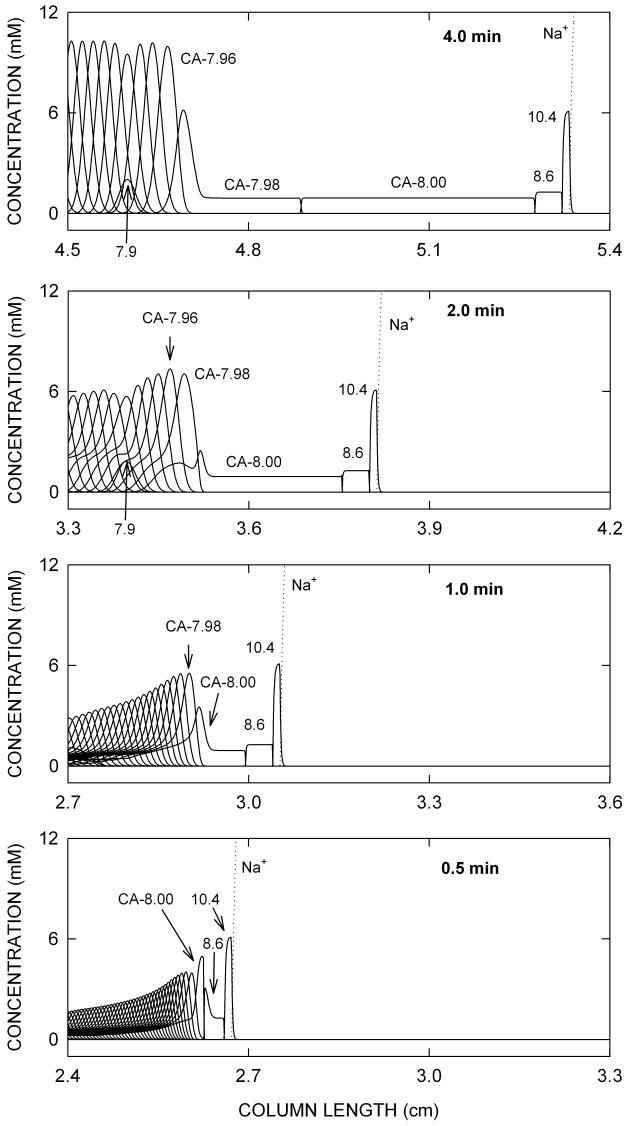

Figure 6: Computer predicted cathodic region showing the distribution of the compounds after 5 min of current application for (A) the case of Figure 1, (B) the same configuration with an additional pI 9.5 spacer compound and (C) with two spacer compounds. CA and S refer to carrier ampholyte and spacer, respectively, and numbers indicate the pI of the components. The cathode is to the right.

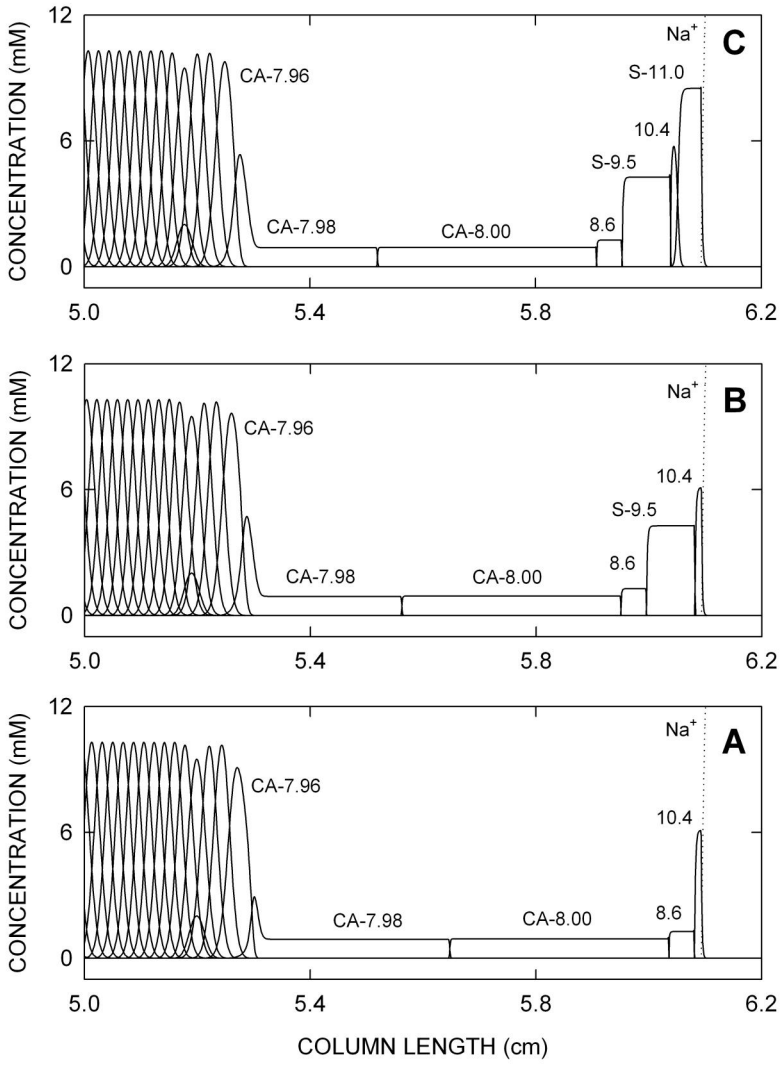

Table 1: Physico-chemical input parameters of sample and buffer components

Compound	pKa_1	pKa_2	Mobility ($x\ 10^{-8}\ m^2/Vs$)	Initial concentration[b] (μM)	Ref.
pI 5.3 analyte	3.70	6.90	2.0	463	37,38
pI 6.4 analyte	4.68	8.12	2.0	398	37,38
pI 6.6 analyte	5.10	8.10	2.0	520	37,38
pI 7.2 analyte	5.70	8.70	2.0	368	37,38
pI 7.9 analyte	6.81	8.99	2.0	329	37,38
pI 8.6 analyte	7.70	9.50	2.0	281	37,38
pI 10.4 analyte	9.50	11.30	2.0	352	37,38
Phosphoric acid [a]	2.00	-	3.67	10'000	30
Cl^-	-	-	7.91	2711	30
Na^+	-	-	5.19	20'000	30
H^+			36.27		30
OH^-			19.87		30

a) Phosphoric acid was treated as monovalent weak acid as it was employed in a low pH environment only.
b) All analytes were sampled as hydrochlorides.